

Kinetics of a frictional granular motor

J. Talbot¹, R. D. Wildman^{1,2} and P. Viot¹

¹ *Laboratoire de Physique Théorique de la Matière Condensée, UPMC, CNRS UMR 7600, 4, place Jussieu, 75252 Paris Cedex 05, France and*

² *School of Mechanical and Manufacturing Engineering, Loughborough University, Loughborough, Leicestershire, LE11 3TU, UK*

(Dated: August 5, 2021)

Within the framework of a Boltzmann-Lorentz equation, we analyze the dynamics of a granular rotor immersed in a bath of thermalized particles in the presence of a frictional torque on the axis. In numerical simulations of the equation, we observe two scaling regimes at low and high bath temperatures. In the large friction limit, we obtain the exact solution of a model corresponding to asymptotic behavior of the Boltzmann-Lorentz equation. In the limit of large rotor mass and small friction, we derive a Fokker-Planck equation for which the exact solution is also obtained.

PACS numbers: 45.70.-n, 45.70.Vn, 05.10.Gg

Recently, Eshuis *et al.* [1], inspired by Smoluchowski's gedankenexperiment, constructed a macroscopic rotational motor consisting of four vanes immersed in a granular gas. When a soft coating was applied to one side of each vane, a ratchet effect was observed above a critical granular temperature. While this was the first experimental realization of a granular motor, similar Brownian ratchets exist in many diverse applications, e.g., photovoltaic devices and biological motors; See [2]. All of these motors share the common features of non-equilibrium conditions and spatial symmetry breaking. Several recent theoretical studies of idealized models of granular motors, which use a Boltzmann-Lorentz description [3–8], show that the motor effect is particularly pronounced when the device is constructed from two different materials, as was the case in the recent experiment [1]. The existing theories, however, predict a motor effect for any temperature of the granular gas while in the experiment the phenomenon is only observed if the bath temperature is sufficiently large. The presence of friction is at the origin of this difference and it is therefore highly desirable to incorporate it in the theoretical schemes.

Several studies have considered the effect of friction on Brownian motion. The pioneering work of de Gennes [9] was motivated by the motion of a coin on a horizontally vibrating plate [10] and a liquid droplet on non-wettable surfaces subjected to an asymmetric lateral vibration; he obtained the stationary velocity distribution, as well as the velocity correlation function. A notable result, obtained independently by Hayakawa [11], is that the Einstein relation no longer holds in the presence of dry friction. More recently, Touchette and coworkers [12–14] obtained a solution of a model with dry friction and viscous damping.

In this Letter, we investigate the kinetic properties of a heterogeneous granular rotor in the presence of dry (Coulomb) friction and we provide exact solutions in the limit of large motor mass (Brownian limit) and also in the limit of strong friction for arbitrary mass.

We consider a two-dimensional system where a hetero-

geneous chiral rotor with moment of inertia I , mass M and the length L immersed in a granular gas at density ρ with a velocity distribution $\phi(v)$ characterized by a granular temperature T . The motor is composed of two materials with coefficients of restitution α_+ and α_- . Collisions of the bath particles, of mass m , with the former (latter) exert a positive (negative) torque. (The experimental setup employed by Eshuis *et al.*, where one has a translational invariance in the third dimension, can also be described by the model).

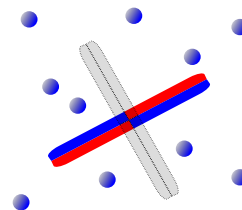


FIG. 1: The chiral rotor is constructed of materials with coefficients of restitution α_+ (red) and α_- (blue). When immersed in a bath of thermalized particles, it acquires a net rotation around its axis. The model can be extended to include additional vanes (shown in gray) as used in the experiment of Eshuis *et al.* [1].

To understand the qualitative effect of the friction, it is useful to consider the torques acting on the rotor: The motor torque is the average of all changes of angular momentum resulting from collisions between the rotor and the bath particles. In the large rotor mass ratio ($M/m \gg 1$), one finds that the motor torque is $(\alpha_+ - \alpha_-) \frac{1}{8} \rho L^2 T$ [15], which vanishes for a symmetric rotor ($\alpha_+ = \alpha_-$) and the dynamic friction is assumed constant and opposed to the motion $-\Gamma_s \sigma(\Omega)$ ($\sigma(\pm x) = \pm 1$, $|x| \neq 0$; $\sigma(0) = 0$). (We neglect static friction in this study, but it will be considered in a future publication). We can define a crossover temperature, $T_c = \frac{8\Gamma_s}{\rho L^2 (\alpha_+ - \alpha_-)}$, that separates a regime dominated by the motor effect ($T > T_c$) and one dominated by friction ($T < T_c$). This mechanical point of view

defining the two kinetic regimes must be expanded by accounting for the fact that the motor torque is a fluctuating quantity.

Assuming the bath is homogeneous, and in the presence of dry friction, the Boltzmann-Lorentz (BL) equation of the angular velocity distribution (AVD), $f(\Omega)$, can be expressed as

$$\frac{\partial}{\partial t} f(\Omega; t) - \frac{\Gamma_s \sigma(\Omega)}{I} \frac{\partial}{\partial \Omega} f(\Omega; t) = J[f, \phi] \quad (1)$$

where the frictional torque Γ_s and $J[f, \phi]$ is the BL collision operator [15]

$$J[f, \phi] = \rho \int_{-\infty}^{\infty} dv \int_{-L/2}^{L/2} d\lambda |v - \lambda \Omega| [\theta(v - \lambda \Omega) \frac{f(\Omega^{**}; t)}{\alpha_+^2} \phi(v^{**}) + \theta(\lambda \Omega - v) \frac{f(\Omega^{**}; t)}{\alpha_-^2} \phi(v^{**})] - \rho \nu(\Omega) f(\Omega; t) \quad (2)$$

with Ω^{**} , v^{**} denoting the pre-collisional velocities, $\theta(x)$ is the Heaviside function and $\rho \nu(\Omega)$ is the total collision rate for a motor rotating at the angular velocity Ω , $\rho \nu(\Omega) = \rho \int_{-\infty}^{\infty} dv \int_{-L/2}^{L/2} d\lambda |v - \lambda \Omega| \phi(v)$. (For a 3D-motor, Eq.1 is unchanged if $\rho = nL_1$, n being the 3D number density and L_1 the perpendicular linear size of the vane.) For convenience we introduce the dimensionless variables $\Omega^* = L\sqrt{\frac{m}{T}}\Omega$, $\Gamma_s^* = \frac{\Gamma_s}{\rho L^2 T}$ and $v^* = v\sqrt{\frac{m}{T}}$. With this choice of units, the steady state angular velocity depends only on α_{\pm} , M/m and Γ_s^* . Also, since the BL description neglects recollisions with the bath particles and is invalid when $M \ll m$, we will assume in the following that $M > m$.

Simulations. A complete analytical treatment of the Boltzmann equation is a very difficult task, even in the steady state. We have performed numerical simulations of the BL equation. (See [16] for details. We note that both in simulation and experiment the sampling time must be smaller than the mean stopping time to avoid biasing the AVD). Fig. 2 shows the dimensionless mean angular velocity Ω^* of an asymmetric rotor ($\alpha_+ = 1$, $\alpha_- = 0$) as a function of a dimensionless dry friction Γ_s^* for different mass ratios $M/m = 1, 2, 10, 20$. As expected, the mean angular velocity decreases as the friction increases. Moreover, two scaling regimes are observed:

$$\langle \Omega^* \rangle \sim \begin{cases} \Gamma_s^{*-1}, & \Gamma_s^* \gg 1 \\ \Gamma_s^*{}^0, & \Gamma_s^* \ll 1 \end{cases} \quad (3)$$

In experiments, the most easily varied parameter is the bath temperature T , and in terms of the original variables, the two scaling regimes correspond to $\langle \Omega \rangle \propto T^{3/2}$ and $\langle \Omega \rangle \sim T^{1/2}$ at low and high temperatures, respectively. (The inset of Fig. 2 shows a log-log plot of the mean angular velocity $\langle \Omega \rangle$ as a function of bath temperature T .)

Limiting Behaviors. We now show that in appropriate limits, the physics can be described by simpler models for

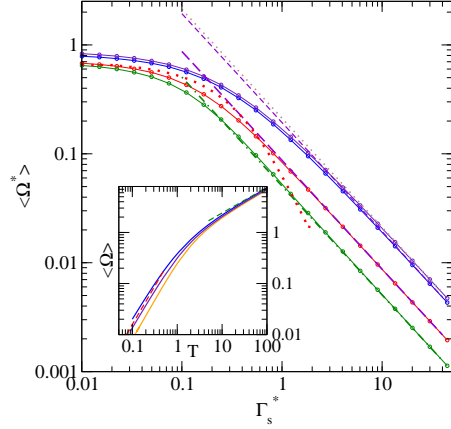


FIG. 2: (Color online) Dimensionless mean angular velocity $\langle \Omega^* \rangle$ of an asymmetric rotor versus Γ_s^* : $\alpha_+ = 1$, $\alpha_- = 0$ for different mass ratios $M/m = 1, 2, 10, 20$, top to bottom obtained from numerical simulations of the BL equation. The dashed and dotted curves correspond to the solutions of the Independent Kick model and the Fokker-Planck equation, respectively. The inset shows $\langle \Omega \rangle$ as a function of the bath granular temperature, T , for $\Gamma_s = 0.2$ and $M/m = 5, 10, 20$. At low temperature $\langle \Omega \rangle \sim T^{3/2}$ and at high temperature $\langle \Omega \rangle \sim T^{1/2}$. The dashed lines are visual guidance for this scaling behavior.

which analytical solutions can be obtained. The analysis is facilitated by considering two time-scales: the average inter-collision time between bath particles and the motor, $\tau_c \simeq \frac{1}{\rho \nu(0)} = \sqrt{\frac{\pi m}{2T}} \frac{1}{\rho L}$ (for a Gaussian bath distribution) and the mean stopping time in the presence of friction, $\tau_s = \frac{I \bar{\Omega}}{\Gamma_s}$ where $\bar{\Omega}$ is the average angular velocity after a collision. When the dimensionless friction Γ_s^* is small, $\bar{\Omega}^* \sim (\alpha_+ - \alpha_-)$, while for $\Gamma_s^* \gg 1$, $\bar{\Omega}^* \sim \frac{mL^2}{I} (\alpha_+ - \alpha_-)$, which gives

$$\frac{\tau_s}{\tau_c} \sim \frac{\alpha_+ - \alpha_-}{\Gamma_s^*} \begin{cases} 1, & \Gamma_s^* \gg 1 \\ \frac{M}{m}, & \Gamma_s^* \ll 1 \end{cases} \quad (4)$$

Whenever slip-stick behavior is present the AVD contains a regular part and a delta singularity at $\Omega^* = 0$ corresponding to a stationary rotor before the next collision with a bath particle:

$$f^*(\Omega^*) = \gamma f_R^*(\Omega^*) + (1 - \gamma) \delta(\Omega^*) \quad (5)$$

where $\int d\Omega^* f_R^*(\Omega^*) = 1$ and γ is a constant that can be determined from conservation of the probability current at $\Omega^* = 0$ [12]:

$$(1 - \gamma) \rho L \int_{-\infty}^{\infty} dv^* |v^*| \phi(v^*) = 2\gamma f_R^*(0) \frac{\Gamma_s^* m L^2}{I} \quad (6)$$

giving $\gamma^{-1} = 1 + 2C \frac{\Gamma_s^* m L^2}{I}$ with $C = 2f_R^*(0) / \int_{-\infty}^{\infty} dy |y| \phi(y)$ is a numerical constant

When $\tau_c \gg \tau_s$ the dry friction stops the motor before the next collision, and the motor essentially evolves by following a sequence of stick-slip motions. Most of the time, the rotor is at rest and the singular contribution is dominant, $\gamma \simeq 1/\Gamma_s^*$. This regime can be described by the Independent Kick model introduced below.

Conversely, when $\tau_c \ll \tau_s$, collisions are so frequent that sliding dominates the motor dynamics. For all practical purposes, the rotor never stops and $(1 - \gamma) \simeq \Gamma_s^*$. In this case, the dynamics is well described by a Fokker-Planck equation for $M/m \gg 1$.

Independent Kick Model. The mean angular velocity is the average over all collisions:

$$\langle \Omega \rangle = \rho \int_{-\infty}^{\infty} dv |v| \phi(v) \int_{-L/2}^{L/2} dx \int_0^{\tau} \Omega(t) dt, \quad (7)$$

where $\Omega(t) = \Omega_0 - \frac{\Gamma_s \sigma(\Omega_0)}{I} t$, $\tau = \frac{|\Omega_0| L}{\Gamma_s}$ and Ω_0 is the angular velocity after a collision, which is given by

$$\Omega_0 = \frac{(1 + \alpha_{\pm}) m x v}{I + m x^2} \quad (8)$$

Integrating over time and x , and by using a Gaussian bath distribution (analytical expressions can be obtained for arbitrary bath distributions, but they are not presented here), the dimensionless mean angular velocity is given by

$$\langle \Omega^* \rangle = \frac{(1 + \alpha_+)^2 - (1 + \alpha_-)^2}{2\Gamma_s^* \sqrt{2\pi}} \left(\frac{\tan^{-1} \sqrt{\xi}}{\sqrt{\xi}} - \frac{1}{1 + \xi} \right) \quad (9)$$

where $\xi = \frac{mL^2}{4I}$. Comparison of the exact expression of the Independent Kick model with the simulation results of the BL equation in Fig. 2 shows that it has the correct dimensionless dependence $1/\Gamma_s^*$.

Finally, the regular part of the AVD can be obtained from the inverse Fourier transform of the characteristic function $\langle e^{ik\Omega} \rangle$. For a Gaussian bath distribution, by using the change of variable $z = 2x/L$, one obtains

$$f_R^*(\Omega^*) = \frac{1}{4\sqrt{2\pi}\xi\gamma\Gamma_s^*} \left[\theta(\Omega^*) \int_0^1 dz e^{-\frac{(1+\xi z^2)^2 \Omega^{*2}}{8\xi^2(1+\alpha_+)^2 z^2}} + \theta(-\Omega^*) \int_0^1 dz e^{-\frac{(1+\xi z^2)^2 \Omega^{*2}}{8\xi^2(1+\alpha_-)^2 z^2}} \right] \quad (10)$$

Therefore, the Independent Kick model provides non-trivial angular velocity distributions which are the sum of a regular function with a non-Gaussian shape, even in the Brownian limit, with an amplitude decreasing as $1/\Gamma_s^*$ and a singular contribution. Fig. 3 a displays regular angular velocity distributions of the BL model for different frictional torques. As expected the amplitude decreases as the friction increases. Fig. 3 b shows the rescaled distributions $\Gamma_s^* \gamma f_R^*(\Omega^*)$ versus Ω^* . One observes that for $\Gamma_s^* > 2$, the curves converge to the AVD of the Independent Kick model, Eq. (10) confirming that it describes very accurately all kinetic properties of the BL model for moderate to large friction.

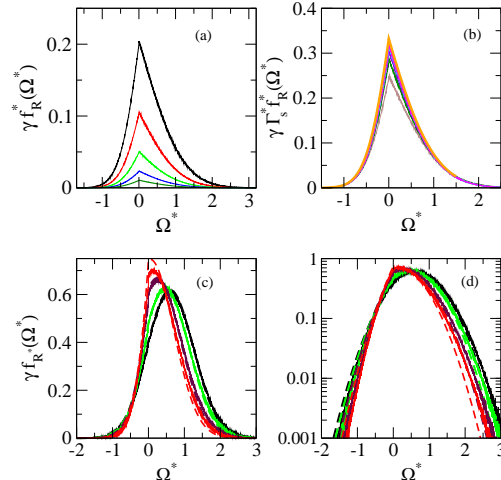


FIG. 3: (Color online) (a) Regular part of the AVD, $\gamma f_R^*(\Omega^*)$, for various frictional torques $\Gamma_s^* = 1.22, 2.72, 6.05, 13.6, 30.0$ (From top to bottom) obtained from numerical simulations of the BL equation. $M/m = 10$ with other parameters the same as in Fig. 2. (b) rescaled $\Gamma_s^* \gamma f_R^*(\Omega^*)$ for the same values of the friction torque (from bottom to top). The upper curve corresponds to Eq.10. (c) AVD $f_R^*(\Omega^*)$ (full curves) and FP solutions (Eq.15, dashed curves) for $M/m = 20$ and $\Gamma_s^* = 0.01, 0.033, 0.074, 0.1$. (d) Log-linear plot of $f_R^*(\Omega^*)$ for the same values of the friction torque.

The amplitude of the singular contribution of $f^*(\Omega^*)$ is given by $1 - \gamma = 1 - \langle e^{ik\Omega^*} \rangle_{k=0} = 1 - \frac{(2+\alpha_++\alpha_-)}{8\xi\Gamma_s^*} \ln(1 + \xi)$. Consequently, the model remains valid if $\gamma < 1$, namely if the frictional torque is sufficiently large. For moderate friction, the Independent Kick model overestimates the mean angular velocity given by the BL equation (see Fig. 2).

Brownian Limit and the Fokker-Planck Equation. We now consider the opposite limit when the stopping time τ_s is much larger than the intercollision time τ_c and when $M \gg m$. For homogeneous granular motors where the mean angular velocity goes to zero in the Brownian limit [3, 17], the Fokker-Planck can be derived by performing a Kramers-Moyal (KM) expansion of the BL integral operator. For heterogeneous granular motors, where the mean angular velocity remains finite, we introduced a KM-like method providing the exact Brownian limit[15], but finite mass corrections cannot be easily included. We propose here an approach that consists of performing a complete series expansion in terms of derivatives of $f(\Omega)$ and a complete resummation of the coefficients allowing the BL operator to be expressed as

$$J[f, \phi] = \sum_{n=1}^{\infty} \frac{1}{n! I^n} \frac{\partial^n (g_n(\Omega) f(\Omega))}{\partial \Omega^n} \quad (11)$$

with $g_n(\Omega) = \left. \frac{\partial^n (g(\Omega, a))}{\partial a^n} \right|_{a=0}$ where the generating function

$g(\Omega, a)$ is given by

$$g(\Omega, a) = 2\rho \int_0^{L/2} dx \int_0^\infty dy y \left[\exp\left(\frac{-(1+\alpha_+)Imxya}{I+mx^2}\right) \phi(x\Omega+y) + \exp\left(\frac{(1+\alpha_-)Imxya}{I+mx^2}\right) \phi(x\Omega-y) \right] \quad (12)$$

Truncating the BL operator, Eq. (11), at second-order and adding the frictional torque leads to the following Fokker-Planck equation

$$\frac{\partial f(\Omega, t)}{\partial t} = \frac{1}{I} \frac{\partial}{\partial \Omega} [(\Gamma_s \sigma(\Omega) + g_1(\Omega))f(\Omega, t)] + \frac{1}{2I^2} \frac{\partial^2}{\partial \Omega^2} [g_2(\Omega)f(\Omega, t)] = 0 \quad (13)$$

in which all finite-mass corrections are incorporated, and where deviations from a Gaussian distribution are present for large finite masses. Recalling that the $g_n(\Omega)$ are proportional to ρ , we see that for a given frictional torque Γ_s , increasing the bath density reduces the effect of friction. The corresponding Langevin equation features a motor torque with a non-linear dependence on Ω and a colored noise.

The steady state solution of Eq. (13) is

$$f(\Omega) = \frac{C_{\Gamma_s}}{g_2(\Omega)} \exp \left[-2I \int_0^\Omega du \left(\frac{g_1(u) + \Gamma_s \sigma(u)}{g_2(u)} \right) \right] \quad (14)$$

where C_{Γ_s} is obtained from the normalization condition $\int d\Omega f(\Omega) = 1$. This result clearly shows that, even in the absence of friction, the AVD is non-Gaussian for finite mass ratios. Moreover, the signature of the presence of friction is a cusp of $f(\Omega)$ at $\Omega = 0$. This feature, also obtained in the Independent Kick model, is always observed in simulation results of the BL equation.

In the Brownian limit $g_1(\Omega) \sim g'_1(\tilde{\Omega})(\Omega - \tilde{\Omega})$ and $g_2(\Omega) = 2T_g g'_1(\tilde{\Omega})$, where T_g (the rotor granular temperature which is lower than the bath temperature, T) and $\tilde{\Omega}$ are given by the Kramers-Moyal expansion (Eqs. 10 and 12 in Ref. [15]). This finally gives a stationary distribution, at the lowest order in m/M ,

$$f(\Omega) = C \exp \left(-\frac{I(\Omega - \tilde{\Omega})^2}{2T_g} - \frac{I\Gamma_s |\Omega|}{g'_1(\tilde{\Omega})T_g} \right) \quad (15)$$

where C is the normalization constant. Whereas one observes a Gaussian decay of the AVD at large velocity, $f(\Omega)$ decreases exponentially for small and intermediate angular velocities, due to the presence of friction. The analytical expression (Eq.15) provides an accurate description of the AVD obtained by simulation (see Fig.3 c and d). A first-order expansion of the dimensionless mean angular velocity can be easily obtained

$$\langle \Omega^* \rangle = (\alpha_+ - \alpha_-)(a_1 - a_2 \Gamma_s^* + \dots) \quad (16)$$

where a_1 and a_2 are positive constants. The dominant term corresponds to the first scaling law obtained in simulation results of the BL equation. More generally, the prediction of the Fokker-Planck equation (dotted curve) is compared to simulation results of the BL equation as a function of the frictional torque Γ_s^* for $M/m = 10$ (see Fig. 2). As expected, the Fokker-Planck description is accurate at low and moderate friction, whereas the Independent Kick model is asymptotically exact in the large friction limit. Even in the small region of moderate frictions Γ^* , the two models slightly overestimate the mean angular velocity. We note that Touchette et al. obtained a time-dependent solution of the FP equation of a particle subject to solid friction and viscous damping [12], corresponding to $\alpha_+ = \alpha_-$ in the present model. This approach can be extended to obtain full solution of the granular Brownian motor.

In their experimental study[1], Eshuis et al. observed that the mean angular velocity increases as $(S - S_c)^{1.4}$ where S is the dimensionless shaking strength and S_c is a threshold value. The relation between $S - S_c$ and T is not clear, but our analysis suggests two scaling laws could be observed in experiments corresponding to the small and large friction limits. Further experiments should clarify this.

We thank Olivier Bénichou for helpful discussions.

-
- [1] P. Eshuis, K. van der Weele, D. Lohse, and D. van der Meer, Phys. Rev. Lett. **104**, 248001 (2010).
 - [2] P. Reimann, Phys. Rep. **361**, 57 (2002).
 - [3] B. Cleuren and C. V. den Broeck, Europhys. Lett. **77**, 50003 (2007).
 - [4] G. Costantini, U. M. B. Marconi, and A. Puglisi, Phys. Rev. E **75**, 061124 (2007).
 - [5] B. Cleuren and R. Eichhorn, J. Stat. Mech. **2008**, P10011 (2008).
 - [6] G. Costantini, U. Marini Bettolo Marconi, and A. Puglisi, Europhys. Lett. **82**, 50008 (2008).
 - [7] G. Costantini, A. Puglisi, and U. Marconi, Eur. Phys. J. Special Topics **179**, 197 (2009).
 - [8] J. Talbot, A. Burdeau, and P. Viot, Phys. Rev. E **82**, 011135 (2010).
 - [9] P. G. de Gennes, J. Stat. Phys. **119**, 953 (2005).
 - [10] A. Buguin, F. Brochard, and P.-G. de Gennes, Eur. Phys. J. E **19**, 31 (2006).
 - [11] H. Hayakawa, Physica D **205**, 48 (2005).
 - [12] H. Touchette, E. V. der Straeten, and W. Just, J. Phys. A: Math. Gen. **43**, 445002 (2010).
 - [13] A. Baule, E. G. D. Cohen, and H. Touchette, J. Phys. A: Math. Gen. **43**, 025003 (2010).
 - [14] A. Baule, H. Touchette, and E. G. D. Cohen, Nonlinearity **24**, 351 (2011).
 - [15] J. Talbot, A. Burdeau, and P. Viot, J. Stat. Mech. **2011**, P03009 (2011).
 - [16] J. Talbot and P. Viot, J. Phys. A: Math. Gen. **39**, 10947

(2006).

[17] J. J. Brey, J. W. Dufty, and A. Santos, *J. Stat. Phys.* **97**, 281

(1999).